Available online at www.sciencedirect.com
ScienceDirect
Quaternary Research 69 (2008) 77–90
QUATERNARY RESEARCH
www.elsevier.com/locate/yqres

Timing of the Nihewan formation and faunas

Chenglong Deng *, Rixiang Zhu, Rui Zhang, Hong Ao, Yongxin Pan

Paleomagnetism and Geochronology Laboratory (SKL-LE), Institute of Geology and Geophysics, Chinese Academy of Sciences, Beijing 100029, China

Received 11 February 2007

Abstract

Magnetostratigraphic dating of the fluvio-lacustrine sequence in the Nihewan Basin, North China, has permitted the precise timing of the basin infilling and associated Nihewan mammalian faunas. The combined evidence of new paleomagnetic findings from the Hongya and Huabaogou sections of the eastern Nihewan Basin and previously published magnetochronological data suggests that the Nihewan Formation records the tectono-sedimentary processes of the Plio–Pleistocene Nihewan Basin and that the Nihewan faunas can be placed between the Matuyama–Brunhes geomagnetic reversal and the onset of the Olduvai subchron (0.78–1.95 Ma). The onset and termination of the basin deposition occurred just prior to the Gauss–Matuyama geomagnetic reversal and during the period from the last interglaciation to the late last glaciation, respectively, suggesting that the Nihewan Formation is of Late Pliocene to late Pleistocene age. The Nihewan faunas, comprising a series of mammalian faunas (such as Maliang, Donggutuo, Xiaochangliang, Banshan, Majuangou, Huabaogou, Xiashagou, Danangou and Dongyaozitou), are suggested to span a time range of about 0.8–2.0 Ma. The combination of our new and previously published magnetostratigraphy has significantly refined the chronology of the terrestrial Nihewan Formation and faunas.

Keywords: Magnetostratigraphy; Magnetochronology; Nihewan Basin; Nihewan Formation; Nihewan faunas

Introduction

The Nihewan Basin (Fig. 1) is located in the transition zone between the North China Plain and the Inner Mongolian Plateau, and covers an area of roughly 150–200 km^2. The basin is filled with Pliocene to Holocene lacustrine, fluvial and wind-blown deposits (Zhu et al., 2003, 2007). The fluvio-lacustrine sequence below the wind-blown sediments has been named the Nihewan Beds (Barbour, 1924). The Nihewan Formation, which represents the type section of the early Pleistocene in North China (Young, 1950), was restricted to the lower portion of the Nihewan Beds. However, in recent studies the name "Nihewan Formation" has been used to define the whole fluvio-lacustrine sequence in the Nihewan Basin (Yuan et al., 1996; Zhu et al., 2007), which was followed in this paper.

Since the 1920s, the basin has attracted the attention of geologists, paleontologists, geochronologists and paleoanthropologists because of its well-developed late Cenozoic strata that are rich in mammalian fossils (known as the Nihewan faunas sensu lato), and its Paleolithic sites (see review by Zhu et al., 2003, 2007; Xie, 2006; Xie et al., 2006). These mammalian fossils traditionally correspond to the Villafranchian fauna in Europe (Barbour, 1925; Teilhard de Chardin and Piveteau, 1930; Qiu, 2000). A series of magnetostratigraphical, sedimentological, geochemical, paleontological and palynological studies (Li and Wang, 1982; Chen, 1988; Schick et al., 1991; Tang et al., 1995; Yuan et al., 1996; Wei, 1997; Qiu, 2000; Løvlie et al., 2001; Zhu et al., 2001, 2003, 2004; Min and Chi, 2003; Wang et al., 2004, 2005, 2006; Deng et al., 2006, 2007) has contributed significantly to our understanding of the complex stratigraphy and depositional systems in the Nihewan Basin, and specifically of early human adaptability to the high northern latitudes in East Asia (Zhu et al., 2001, 2003, 2004, 2007; Wang et al., 2005, 2006; Deng et al., 2006, 2007).

Considerable progress has been made during the past three decades towards paleomagnetically dating the stratigraphy, mammalian fossil localities and Paleolithic sites in this basin. The mammalian faunas in the eastern Nihewan Basin reliably dated by magnetostratigraphy are listed in Table 1. However,

* Corresponding author. Fax: +86 10 6201 0846.
E-mail address: cldeng@mail.iggcas.ac.cn (C. Deng).

0033-5894/$ - see front matter © 2007 University of Washington. All rights reserved.
doi:10.1016/j.yqres.2007.10.006

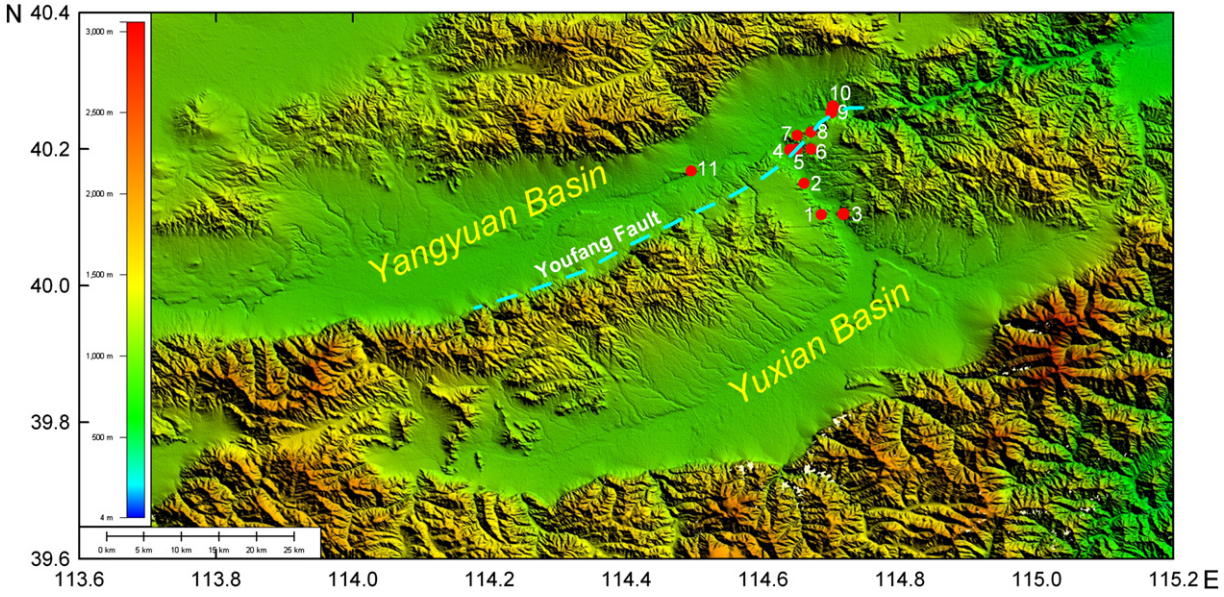

Figure 1. Schematic map showing the eastern Nihewan Basin, the sections (solid circles) mentioned in this paper, and the Youfang fault (dashed line). 1, Huabaogou (HBG); 2, Hongya (HY); 3, Danangou (DNG) and Dongyaozitou (DZ); 4, Donggou (DG); 5, Xiaochangliang (XCL) and Xiantai (XT); 6, Donggutuo (DGT), Maliang (ML), and Feiliang (FL); 7, Haojiatai (HJT); 8, Majuangou (MJG) and Banshan (BS); 9, Shixiali; 10, Xiashagou (XSG); 11, Hutouliang (HTL).

the onset and termination ages of the Nihewan Formation remain an open question. Also, the timing of some important mammalian faunas contained in the formation, such as the Hongya (HY) (Huang and Tang, 1974), Huabaogou (HBG) (Wang, 1982; Zhou et al., 1991), Xiashagou (XSG) (Teilhard de Chardin and Piveteau, 1930), Danangou (DNG) (Li, 1984), and Dongyaozitou (DZ) (Tang, 1980; Tang and Ji, 1983) faunas, is still not precisely constrained. As a result, the chronological sequence of the Nihewan faunas has not yet been established. Here we contribute to the issues with detailed magnetostratigraphic results on two exposed parallel sections of fluvio-lacustrine sediments at HY (40°08.173′N, 114°39.568′E) and HBG (40°06.33′N, 114°41.06′E) (Fig. 1), eastern Nihewan Basin, coupled with a series of published magnetochronology data also obtained in the eastern basin. Our study leads to precise calibration and constraint on the chronological framework of the terrestrial Nihewan Formation and associated faunas.

Magnetostratigraphy of the HY and HBG sections

Geological setting and sampling

HY and HBG sections are located in the western bank of the lower Huliuhe River. The natural outcrops have thicknesses of 126 m and 92 m at HY and HBG, respectively. Both sections are capped by the late Pleistocene or Holocene loess sediments of eolian origin, with thicknesses of 0.2 m and 1.2 m at HY and HBG, respectively. A 3.5-m-deep well was dug to extend the HY paleomagnetic result, which records a depth interval from 126 to 129.5 m. With the exception of the late Pleistocene or Holocene loess sediments, the natural outcrops of the two sections are of fluvio-lacustrine origin. The sediments in the well are red clay of eolian origin. The unconformable contact between the fluvio-lacustrine sequence and the eolian red clay is clearly observed on the walls of the well.

The HY and HBG sections yield three mammalian fossil-bearing sedimentary layers. The HY layer, located at the depth of 114–122 m in the HY section, preserves a mammalian fauna, mainly including *Hipparion* sp. and *Chilotherium* sp. (Huang and Tang, 1974) (Table 1). In the HBG section, there are two layers preserving rich mammalian faunas. The fauna at HBG-I (74–80 m depth) includes *Postschizotherium* sp., *Hipparion houfenense*, *Viverra* sp., *Gazella blacki*, *Antilospiroides hobeiensis*, *Sinoryx* sp. and *Gazella* sp. (Wang, 1982; Zhou et al., 1991) (Table 1); and that at HBG-II (83–90 m depth) includes Leporidae gen. et sp. indet., *Canis* sp., *Canis multicuspus*, *Nyctereutes sinensis*, *Hipparion* cf. *hippidiodus*, *Hipparion* sp., *Palaeotragus* sp., *Gazella* sp. and *Gazella blacki* (Wang, 1982) (Table 1).

In this study, we paleomagnetically sampled the HY and HBG sections. Sampling intervals in the HY natural outcrop and in the well at the bottom of the HY section were, respectively, ~0.4 m and 0.2 m. A total of 294 oriented block samples were taken from the HY section. Sampling interval in the HBG section is ~0.4 m, and 185 oriented block samples were collected. Cubic specimens of 20×20×20 mm were obtained from those block samples in the laboratory.

Mineral magnetic measurements

High-temperature magnetic susceptibilities (χ–T curves) were measured on selected samples using a KLY-3 Kappabridge with a CS-3 high-temperature furnace (Agico Ltd., Brno). There are two types of χ–T curves for the representative samples of the fluvio-lacustrine sediments from the HY and HBG sections (Fig. 2). One is characterized by a major drop in magnetic susceptibility at about 585°C (Figs. 2a–c and g–l), the Curie

https://doi.org/10.1016/j.yqres.2007.10.006 Published online by Cambridge University Press

point of stoichiometric magnetite; the other, characterized by a major drop in magnetic susceptibility at about 620°C (Figs. 2d–f), the feature of partially-oxidized magnetite. These behaviors indicate that both stoichiometric and partially-oxidized magnetites are the major contributors to the magnetic susceptibility.

Table 1
List of mammalian faunas in the eastern Nihewan Basin directly dated by magnetostratigraphy

Taxa	DGT[a]	ML[b]	XCL[c]	MJG-III[d]	BS[e]	HY[f]	HBG-I[g]	HBG-II[h]
Allophaiomys cf. *A. pliocaenicus*			+					
Antilospiroides hobeiensis							+	
Bison sp.	+							
Bovinae indet.			+					
Canis sp.	+				+			+
Canis multicuspus								+
Carnivora gen. et sp. indet.				+				
Cervus sp.			+	+				
Chilotherium sp.						+		
Coelodonta antiquitatis	+	+	+	+	+			
Elephas sp.				+				
Equus sanmeniensis	+		+	+				
Equus sp.		+			+			
Gazella sp.	+		+	+			+	+
Gazella blacki							+	+
Hipparion sp.			+			+		+
Hipparion houfenense							+	
Hipparion cf. *hippidiodus*								+
Pachycrocuta licenti			+					
Pachycrocuta sp.				+				
Leporidae gen. et sp. indet.								+
Martes sp.			+					
Mimomys chinensis			+					
Myospalax cf. *fontanieri*	+							
Nyctereutes sinensis								+
Palaeoloxodon sp.	+	+	+					
Palaeotragus sp.								+
*Postschizotherium*sp.							+	
Proboscidipparion sinensis			+					
Sinoryx sp.							+	
Struthio sp.				+				
Viverra sp.							+	

[a] DGT (Wei, 1985, 1991), ~1.1 Ma (Li and Wang, 1982; Wang et al., 2005).
[b] ML (Wei, 1991), ~0.8 Ma (Wang et al., 2005).
[c] XCL (You et al., 1980; Tang et al., 1995), 1.36 Ma (Zhu et al., 2001).
[d] MJG-III (Zhu et al., 2004), 1.66 Ma (Zhu et al., 2004).
[e] BS (Wei, 1994), 1.32 Ma (Zhu et al., 2004).
[f] HY (Huang and Tang, 1974), 1.95–2.58 Ma (this study).
[g] HBG-I (Wang, 1982; Zhou et al., 1991), 1.07–1.77 Ma (this study).
[h] HBG-II (Wang, 1982), 1.77–1.95 Ma (this study). See the caption of Figure 1 for acronyms of the sections.

Most of the selected samples exhibit heating curves with a more or less pronounced susceptibility hump at 250°–300°C. The steady increase of susceptibility below 250°–300°C may be ascribed to the gradual unblocking of fine-grained (near the superparamagnetic/single-domain boundary) ferrimagnetic particles (Deng et al., 2005; Wang et al., 2005). Hematite, which is another important carrier of the natural remanence suggested by the progressive thermal demagnetization analyses, is not well expressed in the χ–T curves because its weak susceptibility is masked by the much stronger contributions of magnetite.

Hysteresis loops were measured on selected samples using a MicroMag 2900 alternating gradient magnetometer (Princeton Measurements Corp., USA). Most of the selected samples show the hysteresis loops closed above 200–250 mT (Figs. 3a–c and f–i), which is consistent with the presence of a dominant ferrimagnetic phase. Some samples show the hysteresis loops closed above 300 mT (e.g., Figs. 3d and e), indicative of the presence of high-coercivity components, e.g., partially-oxidized coarse-grained magnetite and/or antiferromagnetic hematite. The hysteresis ratios (M_{rs}/M_s versus B_{cr}/B_c) (Day et al., 1977) indicate that the average magnetic grain size falls in pseudo-single domain range.

Demagnetization of the natural remanent magnetization (NRM)

Remanence measurements were made using a 2G Enterprises Model 760-R cryogenic magnetometer installed in a magnetically shielded space (<300 nT). Firstly, 432 samples were subjected to progressive thermal demagnetization (12–19 steps) up to a maximum temperature of 680°C, with 25°–50°C interval below 585°C and 10°–15°C above 585°C, using a magnetic measurements thermal demagnetizer with a residual magnetic field less than 10 nT. Secondly, forty-seven sandy samples, which did not give reliable characteristic remanent magnetization (ChRM) directions by thermal demagnetization, were subjected to a 150°C thermal demagnetization followed by alternating field (AF) demagnetization at peak fields of up to 60 mT. Both methods were capable of isolating the ChRMs after the removal of soft secondary component of magnetization.

Demagnetization results were evaluated by orthogonal diagrams (Zijderveld, 1967), and the principal components direction was computed by a "least-squares fitting" technique (Kirschvink, 1980). Representative demagnetization diagrams are shown in Figures 4 and 5. Generally, a secondary magnetic component, probably of viscous origin, was present and was removed by thermal demagnetization at 200°C. For most samples, the high-stability ChRM component was separated between 250° and 585°C (e.g., Figs. 4a, e and f). However, for some samples, the high-stability ChRM component persists up to 680°C (e.g., Figs. 5a and b) or up to 60 mT (Figs. 4b and c). The behaviors indicate that both magnetite and hematite dominate the remanence carriers in the HY and HBG fluvio-lacustrine sediments. A total of 305 (71%) and 26 (55%) samples gave reliable characteristic remanence directions with thermal and AF demagnetization, respectively. The virtual geomagnetic pole (VGP) latitudes were calculated from the ChRM data to construct the magnetostratigraphy for the two sections.

https://doi.org/10.1016/j.yqres.2007.10.006 Published online by Cambridge University Press

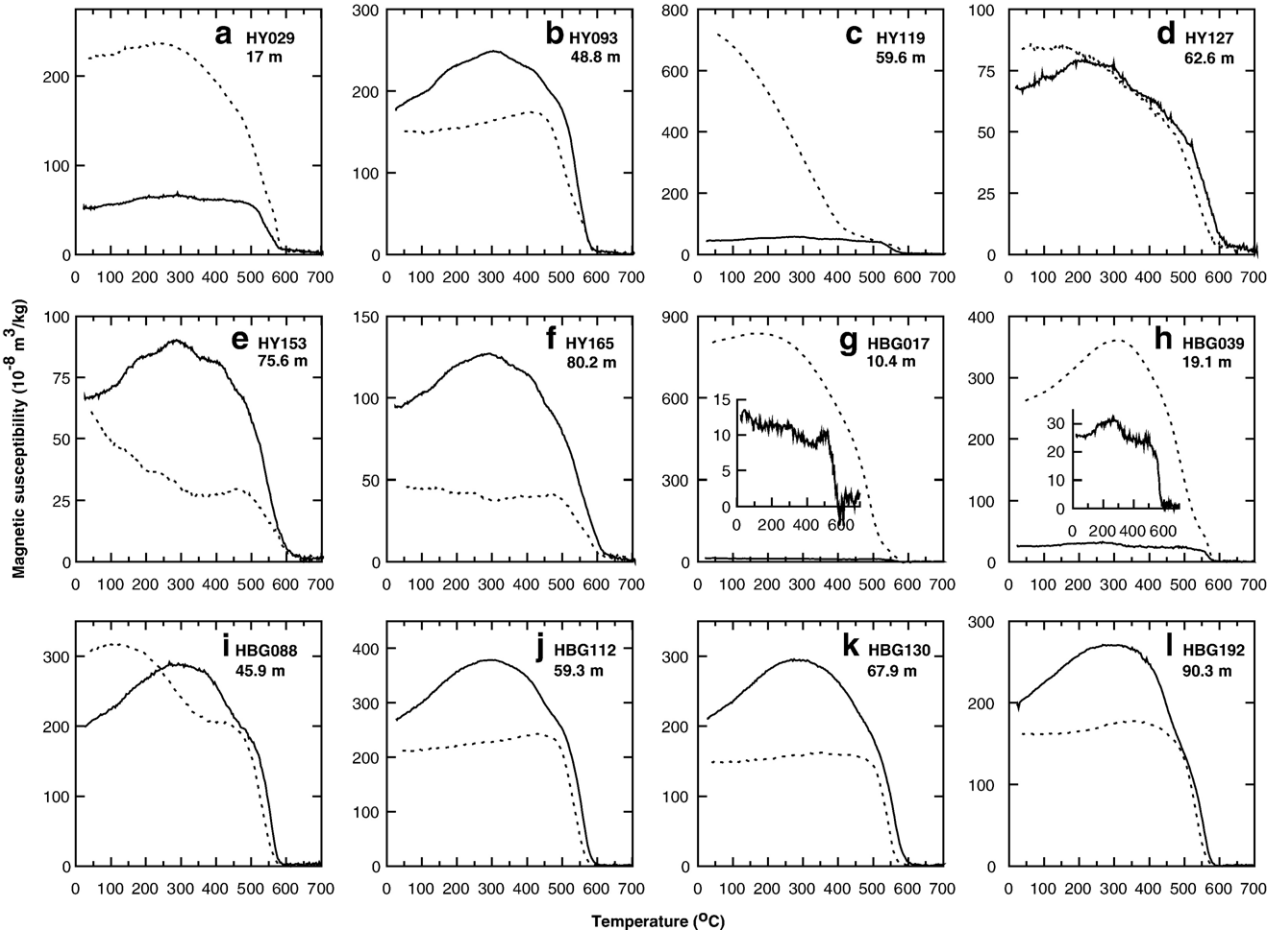

Figure 2. High-temperature magnetic susceptibility (χ–T) of selected samples of the HY (a–f) and HBG (g–l) sections. Solid lines represent heating curves; dotted lines represent cooling curves. The insets in panels g and h show the heating curves only.

Magnetic polarity stratigraphy of the HY and HBG sections

Following demagnetization, eight magnetozones are recognized at the HY section (Fig. 6): four normal, N1 (0–18.8 m), N2 (35.8–39.1 m), N3 (76.3–110.3 m) and N4 (122.8–127.7 m); and four reverse, R1 (18.8–35.8 m), R2 (39.1–76.3 m), R3 (110.3–122.8 m) and R4 (127.7–129.4 m). Six magnetozones are recognized at the HBG section (Fig. 7): three normal, N1 (3.85–34 m), N2 (41.6–51.5 m) and N3 (80–89.2 m); and three reverse, R1 (34–41.6 m), R2 (51.5–80 m) and R3 (89.2–91.7 m). In addition, two short intervals of possible transitional field behavior, labeled e1 and e2 in Figure 6, are recorded within magnetozone R2 at HY (e1: 56.6–57.4 m and e2: 62.8–65.1 m).

On the basis of the paleomagnetic and sedimentological data, the HY (Fig. 6) and HBG (Fig. 7) magnetozones can be correlated with the geomagnetic polarity timescale (Berggren et al., 1995). The late Pleistocene or Holocene loess sediments were found to overlay the fluvio-lacustrine successions of the two sections (Figs. 6a and 7a), and typical red clay of eolian origin and Pliocene age (Ding et al., 1998) underlay the HY section (Fig. 6a). Hence, the overlying late Pleistocene or Holocene loess sediments and underlying Pliocene red clay provide robust geochronological constraint on the HY and HBG fluvio-lacustrine sequences. As a result, HY and HBG magnetozones N1, N2 and N3 correspond to the Brunhes chron, the Jaramillo subchron and the Olduvai subchron, respectively, and HY magnetozone N4 corresponds to the late Gauss chron.

However, it is difficult to estimate the ages of the two geomagnetic excursions determined in HY magnetozone R2 (Fig. 6f) due to vertical facies variation. In addition, we note that the average sedimentation rates of magnetozones N3 (18.89 cm ka^{-1}), R3 (1.98 cm ka^{-1}) and N4 (1.07 cm ka^{-1}) of the HY section are variable. This high variability in sedimentation rates is ubiquitous in the continental fluvio-lacustrine sequences of the eastern Nihewan Basin (Deng et al., 2007), possibly due to local faulting activities or major changes of sedimentary environments.

Magnetochronology of the Nihewan Formation and faunas

Age of the Nihewan Formation

Our new paleomagnetic finding, coupled with sedimentological data, indicates that the fluvio-lacustrine sequences in the eastern Nihewan Basin were deposited from the late Gauss chron into the late Brunhes chron. Typical red clay of eolian origin was found at the bottom of the HY section, where the Matuyama–Gauss geomagnetic reversal is determined within the bottom of

https://doi.org/10.1016/j.yqres.2007.10.006 Published online by Cambridge University Press

the Nihewan fluvio-lacustrine sequence, 1.7 m above the eolian red clay formation (Fig. 6). Therefore, it can be safely concluded that the basal age of the Nihewan Formation at least in the eastern Nihewan Basin (Fig. 1) is constrained to just prior to the Matuyama–Gauss geomagnetic reversal, that is, between ~2.6 and ~3.0 Ma.

The fluvio-lacustrine sequences in the eastern Nihewan Basin record not only the coarse magnetostratigraphy since the Late Pliocene (Fig. 8) (that is, the late Gauss chron, the Matuyama and Brunhes chrons, and the Jaramillo and Olduvai subchrons (Zhu et al., 2001, 2003, 2004; Wang et al., 2004, 2005, 2006; Deng et al., 2006, 2007)) but also some of the fine structures, such as the Punaruu and Cobb Mountain geomagnetic events (Wang et al., 2004; Zhu et al., 2004) and possible Kamikatsura or Santa Rosa events (Wang et al., 2005; Deng et al., 2006). Therefore, our new and previously published paleomagnetic findings have placed stringent chronological controls on the Nihewan Beds that were originally reported over 80 yr ago (Barbour, 1924) and that are now collectively named the Nihewan Formation.

The Nihewan Formation records the tectono-sedimentary processes of the Plio–Pleistocene Nihewan Basin (Fig. 9). The onset of basin deposition was a result of tectonic down-faulting during the Late Pliocene (Zhou et al., 1991). The Youfang dip-slip fault (Fig. 1), which can be clearly observed between the Xiaochangliang (XCL) and Majuangou (MJG) Paleolithic sites (Figs. 9a and c) appears to have played a major role in the formation of the Nihewan paleolake. Although precise timing of activity along the Youfang dip-slip fault remains unsettled, the presence of an ~30-m vertical fault displacement in the early Pleistocene fluvio-lacustrine sediments, observed just below the XCL Paleolithic site, is indicative of an episode of the activity of the Youfang dip-slip fault during the Pleistocene.

Infilling process of the eastern Nihewan Basin

The combined magnetochronology has provided an insight into the infilling process of the eastern Nihewan Basin. During the Pliocene, typical red clay of eolian origin was accumulated not only in the Chinese Loess Plateau (Ding et al., 1998) but also in the area of today's Nihewan Basin. The red clay formation serves as the underlying sediment of the fluvio-lacustrine Nihewan Formation. For example, it can now be found in the

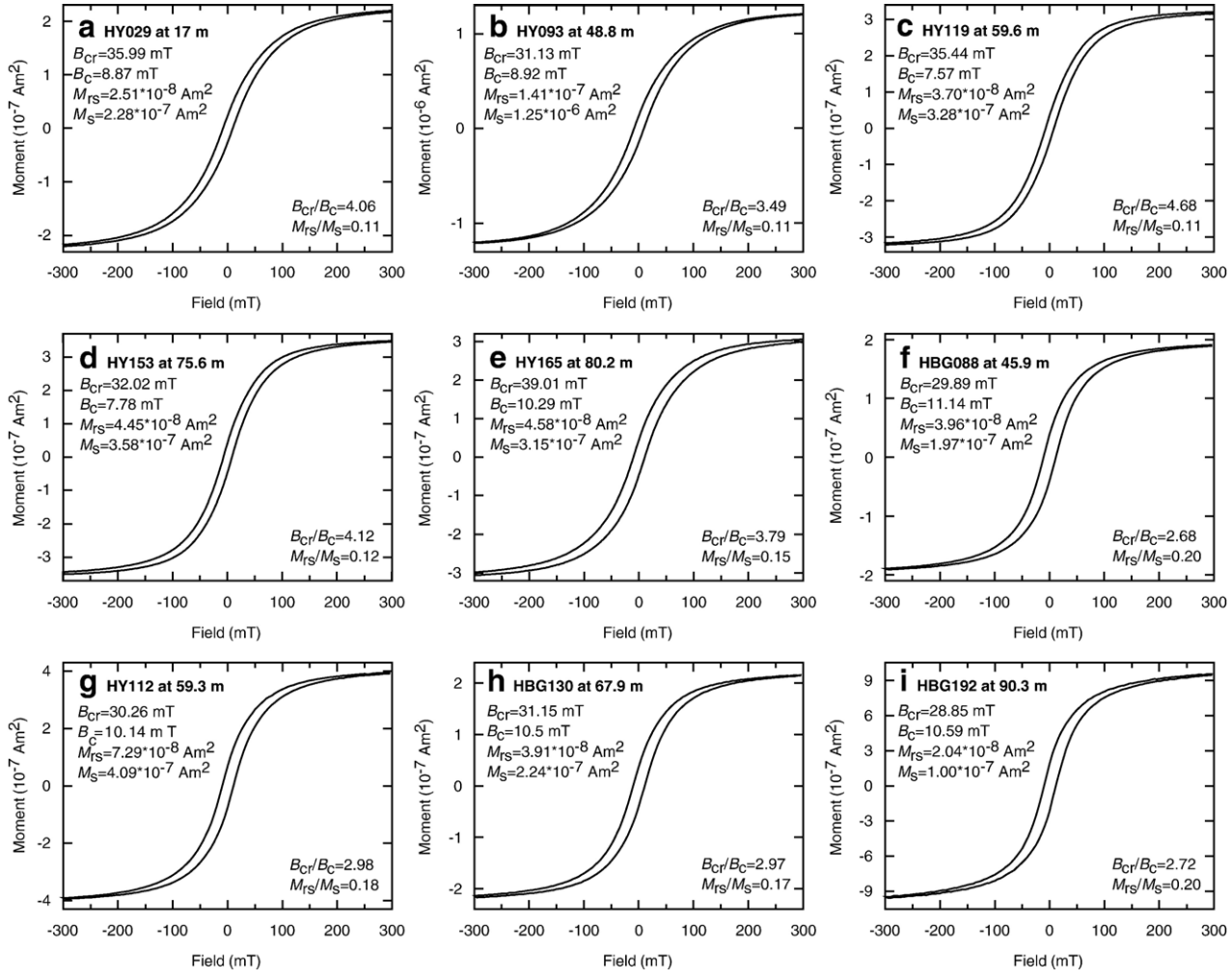

Figure 3. Hysteresis loops for representative samples of the HY (a–e) and HBG (f–i) sections after slope correction for paramagnetic contribution. The hysteresis loops were measured in fields up to ±1.0 T.

https://doi.org/10.1016/j.yqres.2007.10.006 Published online by Cambridge University Press

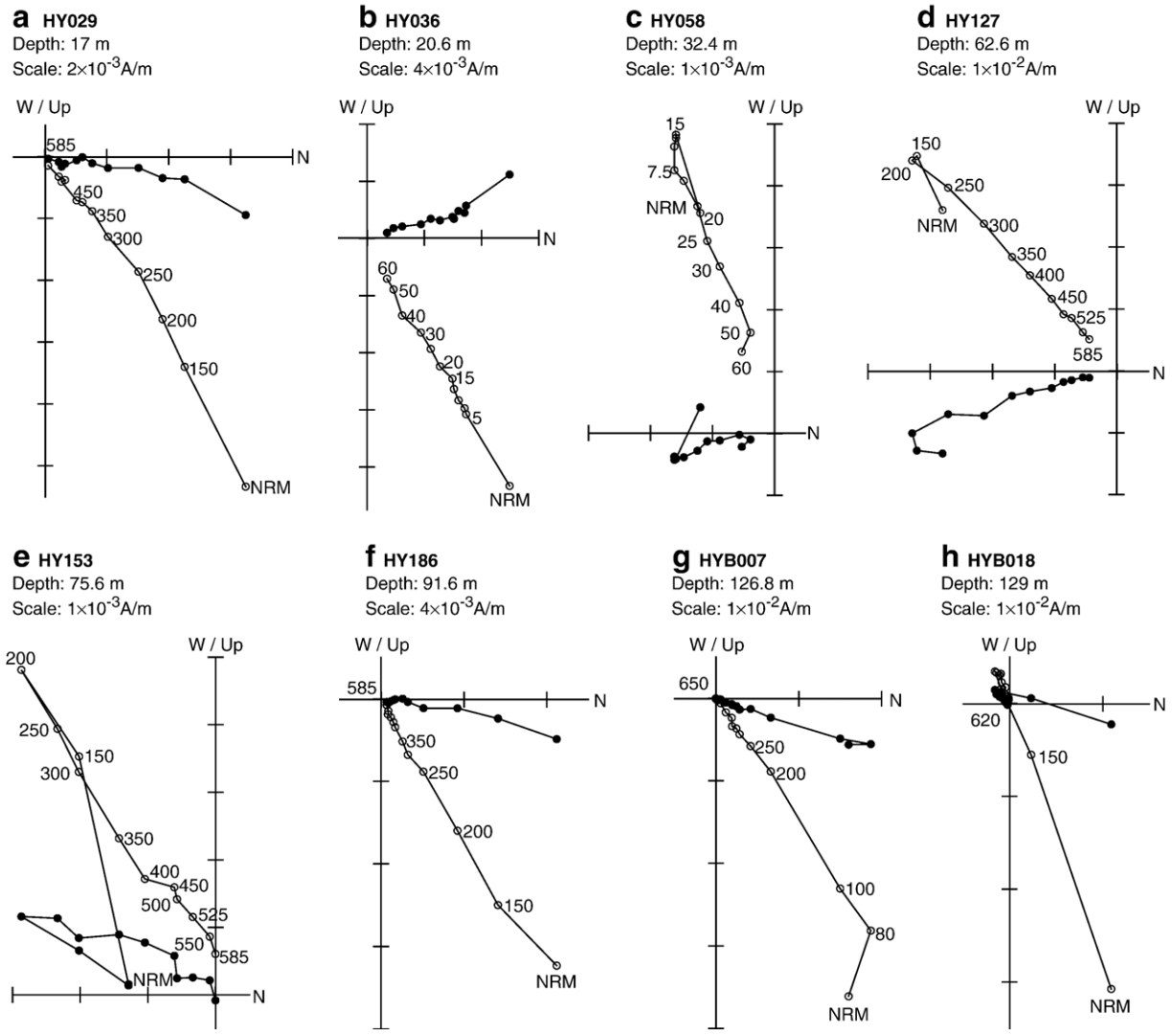

Figure 4. Orthogonal projections of representative progressive thermal (a, d–h) and alternating field (b, c) demagnetization of the HY section. Samples HY036 (b) and HY058 (c) were subjected to a 150°C thermal demagnetization followed by alternating field (AF) demagnetization at peak fields up to 60 mT. The solid (open) circles represent the horizontal (vertical) planes. The numbers refer to the temperatures in °C (a, d–h) or alternating fields in mT (b, c). NRM is the natural remanent magnetization.

well dug at the bottom of the HY section (Fig. 6a). The termination of the Kaena reverse polarity subchron, with an age of 3.04 Ma (Berggren et al., 1995), was recorded in the upper part of the red clay formation (Fig. 6).

Deposits of the Nihewan Formation in fluvio-lacustrine environments followed the eolian red clay formation. At HY and HBG, the Nihewan Formation can be divided into two parts: an upper part, consisting of grayish-green and grayish-yellow silts intercalated with conglomerate and calcareous layers, and a lower part comprising red silts intercalated with conglomerate layers and conglomeratic red silts (Figs. 8h, i and 9d). The stratigraphic boundary between the two parts is located at 93-m depth in the HY section (Fig. 8h) and at 52-m depth in the HBG section (Figs. 8i and 9d). This difference may be due to local faulting. The upper part of grayish-green and grayish-yellow colors has been claimed to represent the early Matuyama chron (Flynn et al., 1997). The lower part of red color was correlated with the late Gilbert chron and the early Gauss chron (Flynn et al., 1997), which was regarded as the red clay formation by Barbour et al. (1927), corresponding to the so-called "*Hipparion* red clay" in the Chinese Loess Plateau (Teilhard de Chardin and Young, 1930).

Our new magnetostratigraphic results significantly refine the geochronology of the sedimentary sequences at HY and HBG. The red clay formation in the Loess Plateau containing *Hipparion* is of eolian origin (Ding et al., 1998). However, the lower part of the HY and HBG sections is of fluvio-lacustrine origin. Our magnetostratigraphic investigation indicates that the red sediments were mainly accumulated during the Matuyama chron (Figs. 6–8), and that the stratigraphic boundary between the two parts mentioned above is found within the Olduvai subchron at HY (Fig. 8h) and just below the Jaramillo subchron at HBG (Fig. 8i), respectively. Prior to the initiation of the Nihewan paleolake, the red clay of eolian origin was deposited in today's Nihewan Basin during the Pliocene. During the late Gauss chron, the development of the Nihewan paleolake was initiated

https://doi.org/10.1016/j.yqres.2007.10.006 Published online by Cambridge University Press

due to fault-controlled subsidence, and the eolian red clay at nearby sources of high relief was reworked and then redeposited. Today, the reworked red sedimentary sequence is found to overlie the eolian red clay formation at some locations, such as at HY and Shixiali (40°14.851′N, 114°42.677′E), or to directly overlie the Mesozoic volcanic rock elsewhere, such as at Xiantai (XT) (Fig. 8d; Deng et al., 2006, Fig. 7). However, the reworked red sedimentary sequence is absent at some locations (e.g., XCL, Feiliang (FL) and Donggutuo (DGT)) or probably inaccessible elsewhere (e.g., MJG, Haojiatai (HJT) (Figs. 8e and f; Zhu et al., 2004, Fig. 2) and Donggou (DG) (Fig. 8g; Zhu et al., 2001, Fig. 3)).

The Nihewan Formation mainly comprises grayish-green, grayish-yellow silts (at DGT, FL, XCL, XT, DG and HJT) and red silts (at HY and HBG) of fluvio-lacustrine origin, which are interbedded with yellow fine-grained sands (at DGT, FL, XCL, XT, DG and HJT) or conglomerates and conglomeratic red silts (at HY and HBG) (Fig. 8). The fluvio-lacustrine sequence is capped by the last interglacial soil and the last glacial loess at HJT, DG, XCL, XT and DGT (Fig. 8) and Shixiali (Fig. 9b), or by the late Pleistocene or Holocene loess sediments at HY, HBG (Fig. 8), and Hutouliang (HTL) (see Fig. 1 for locations of the sections). These observations indicate that the drying up of the Nihewan paleolake commenced during the last interglacial period at HJT and nearby sections, and that the ultimate disappearance of the paleolake at HY, HBG and HTL occurred probably during the late last glaciation.

Age of the Nihewan faunas

The mammalian faunas assessed in this paper include those with reliable magnetochronological constraints, such as DGT (Wei, 1985, 1991), Maliang (ML) (Wei, 1991), XCL (You et al., 1980; Tang et al., 1995), Banshan (BS) (Wei, 1994), MJG-III (Zhu et al., 2004), HY (Huang and Tang, 1974), HBG-I (Wang, 1982) and HBG-II (Wang, 1982; Zhou et al., 1991) faunas

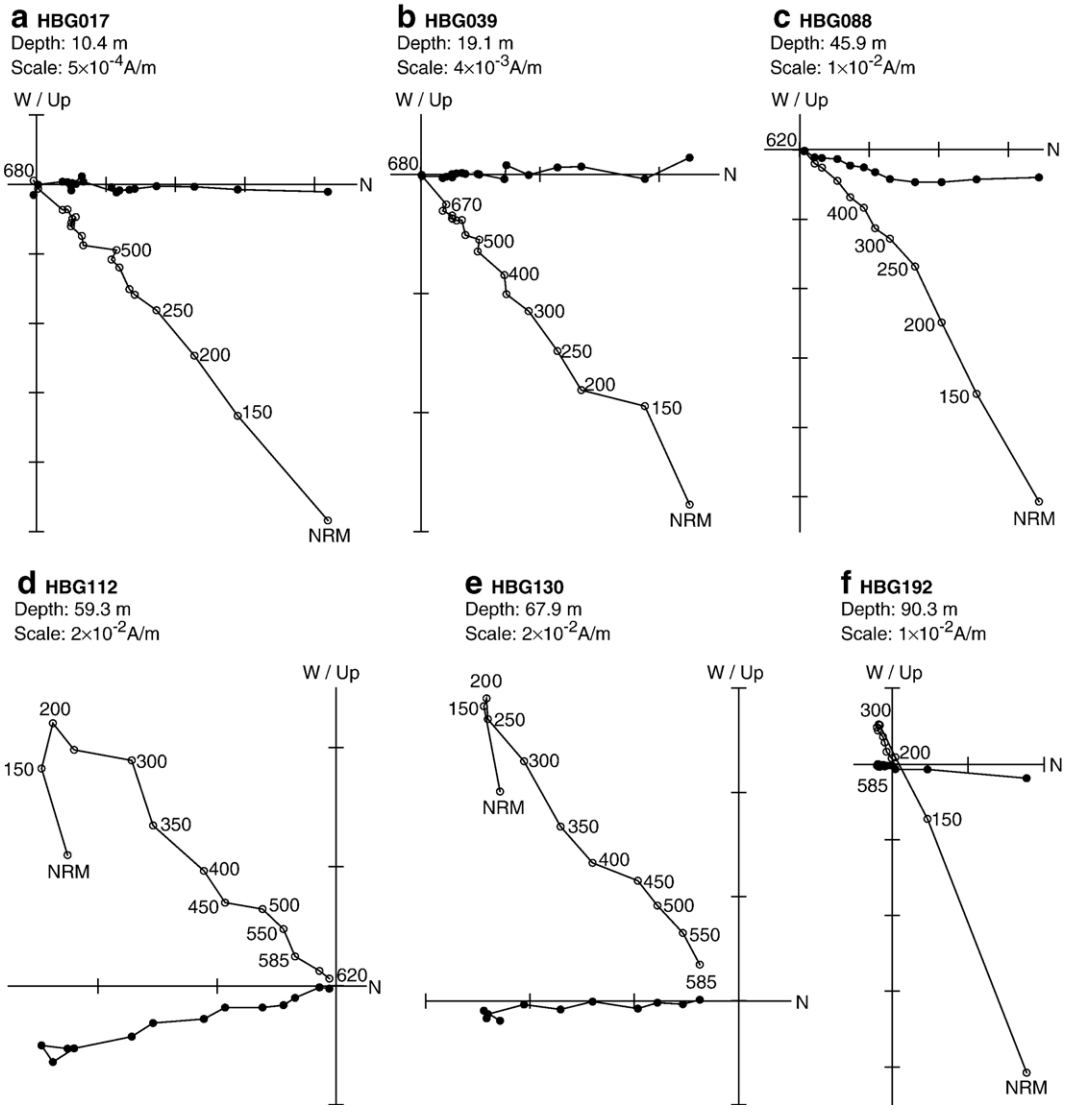

Figure 5. Orthogonal projections of representative progressive thermal demagnetization of the HBG section. The solid (open) circles represent the horizontal (vertical) planes. The numbers refer to the temperatures in °C. NRM is the natural remanent magnetization.

https://doi.org/10.1016/j.yqres.2007.10.006 Published online by Cambridge University Press

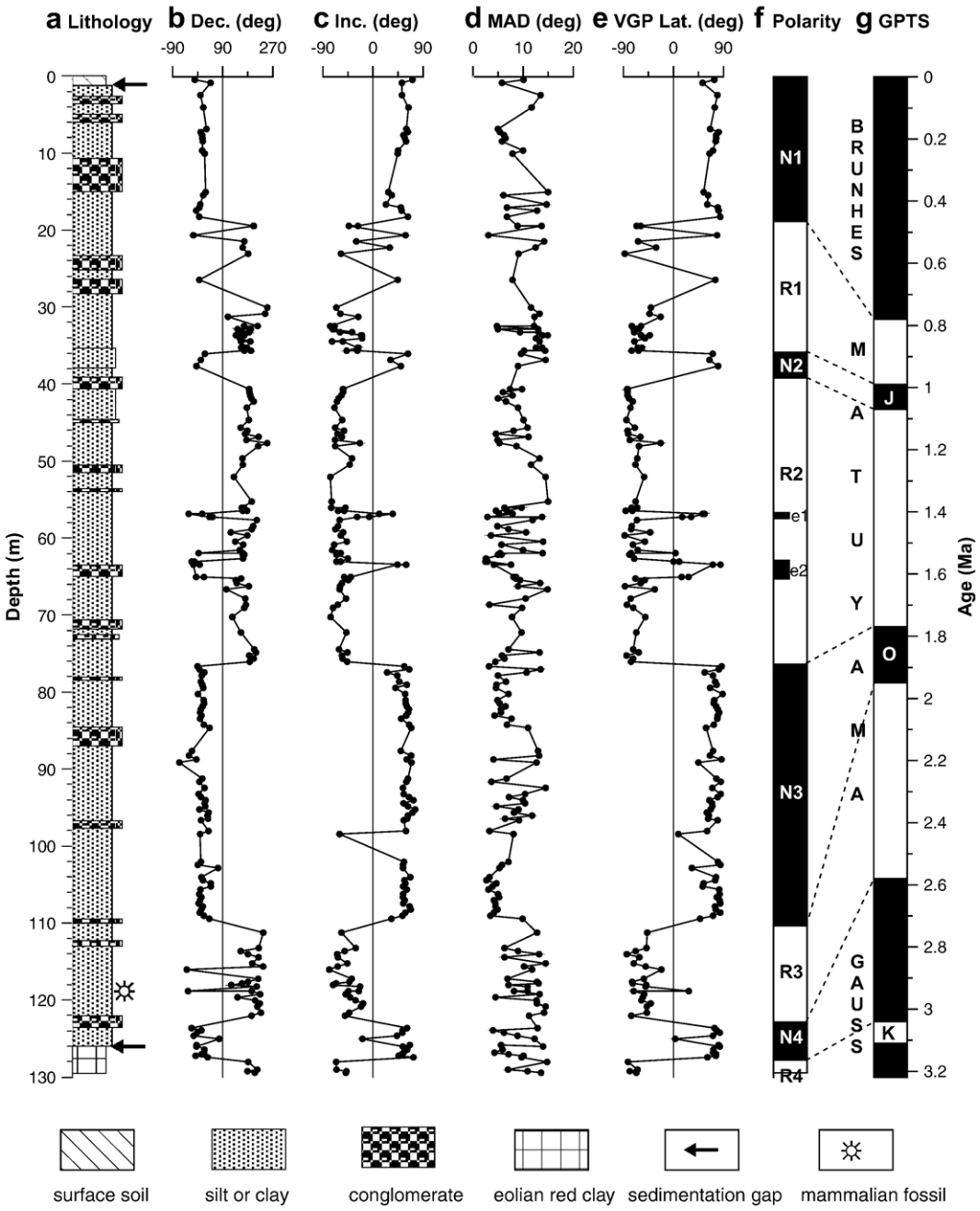

Figure 6. Lithostratigraphy and magnetostratigraphy of the HY section. (a) Lithology. (b) Declination (Dec.). (c) Inclination (Inc.). (d) Maximum angular deviation (MAD). (e) Virtual geomagnetic pole (VGP) latitude. (f) Magnetic polarity zonation. (g) Geomagnetic polarity timescale (GPTS) (Berggren et al., 1995). J, Jaramillo; O, Olduvai; K, Kaena. Note that the section is capped by the late Pleistocene or Holocene loess sediments, and note the sedimentation gap between the fluvio-lacustrine sequence and the eolian red clay.

(Table 1, Fig. 8), and those without independent age constraints, such as XSG (Teilhard de Chardin and Piveteau, 1930), DNG (Li, 1984) and DZ (Tang, 1980; Tang and Ji, 1983) faunas. Most of the stratigraphic sequences bearing those faunas have been magnetostratigraphically investigated in our present (Figs. 6 and 7) and recent (Zhu et al., 2001, 2003, 2004; Wang et al., 2005) studies. Therefore, our detailed magnetostratigraphic dating of the fossiliferous Nihewan Formation offers an excellent opportunity to independently constrain the chronology of the mammalian faunas. Although there are no magnetochronological data from XSG, DNG and DZ faunas, which are important components of the Nihewan faunas, our magnetostratigraphic framework could provide a robust chronological control for intrabasin correlation and calibration of all the faunas in the Nihewan Basin based on faunal similarity.

The new magnetostratigraphic results presented in this study significantly revise the chronology of the HY, HBG-I and HBG-II faunas, which show that the HY fauna is located in the pre-Olduvai Matuyama chron (Figs. 6 and 8h), and that the HBG-I and HBG-II faunas are located in the post-Olduvai Matuyama chron and within the Olduvai subchron, respectively (Figs. 7 and 8i). Our previously published magnetostratigraphic data

https://doi.org/10.1016/j.yqres.2007.10.006 Published online by Cambridge University Press

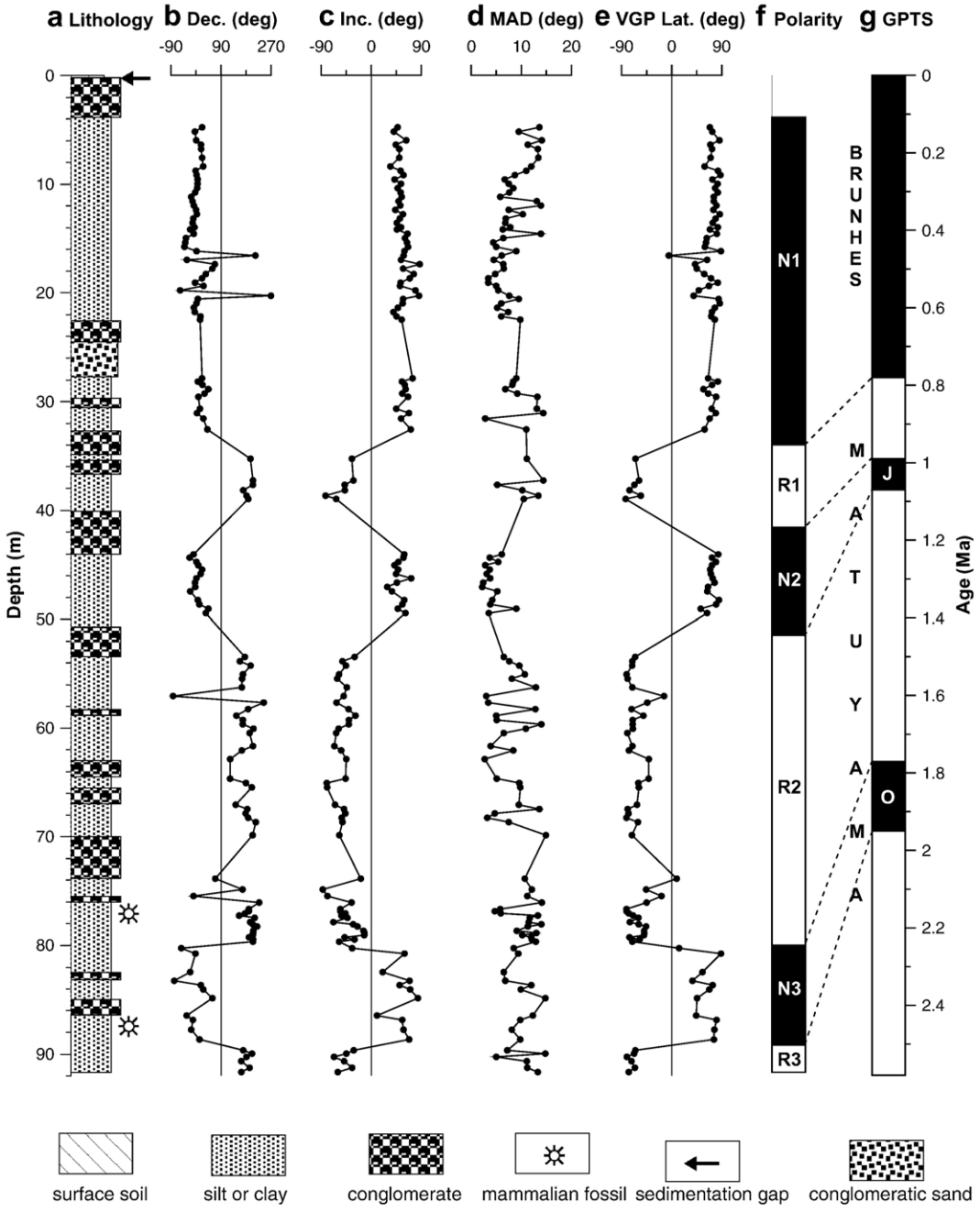

Figure 7. Lithostratigraphy and magnetostratigraphy of the HBG section. (a) Lithology. (b) Declination (Dec.). (c) Inclination (Inc.). (d) Maximum angular deviation (MAD). (e) Virtual geomagnetic pole (VGP) latitude. (f) Magnetic polarity zonation. (g) Geomagnetic polarity timescale (GPTS) (Berggren et al., 1995). J, Jaramillo; O, Olduvai. Note that the section is capped by the late Pleistocene or Holocene loess sediments.

(Zhu et al., 2001, 2004; Wang et al., 2005) have suggested that the faunas of MJG-III, BS, XCL and DGT reside in the Matuyama chron bracketed by the Olduvai and Jaramillo subchrons (Figs. 8b, c and e), and that the ML fauna is located just below the Matuyama–Brunhes boundary (Fig. 8b). More precisely, the DGT fauna is located just below the lower boundary of the Jaramillo subchron (Fig. 8b), and the MJG-III fauna is fairly closed to the upper boundary of the Olduvai subchron (Fig. 8e).

The faunas listed above are placed between the Matuyama–Brunhes and Gauss–Matuyama geomagnetic reversals, that is, between 0.78 Ma and 2.58 Ma. Considering that only two species were found in the HY mammalian locality (Huang and Tang, 1974), the locality is excluded when we address the chronology of the Nihewan faunas in this study. We conclude that the typical Nihewan faunas (see Table 1) occur between the Matuyama–Brunhes geomagnetic reversal and the onset of the Olduvai subchron (Fig. 8), that is, between 0.78 Ma and 1.95 Ma.

The famous XSG fauna, which yields a rich faunal list (Table 2), was also named the Nihewan Fauna (sensu stricto) (Teilhard de Chardin and Piveteau, 1930). Of those faunal

https://doi.org/10.1016/j.yqres.2007.10.006 Published online by Cambridge University Press

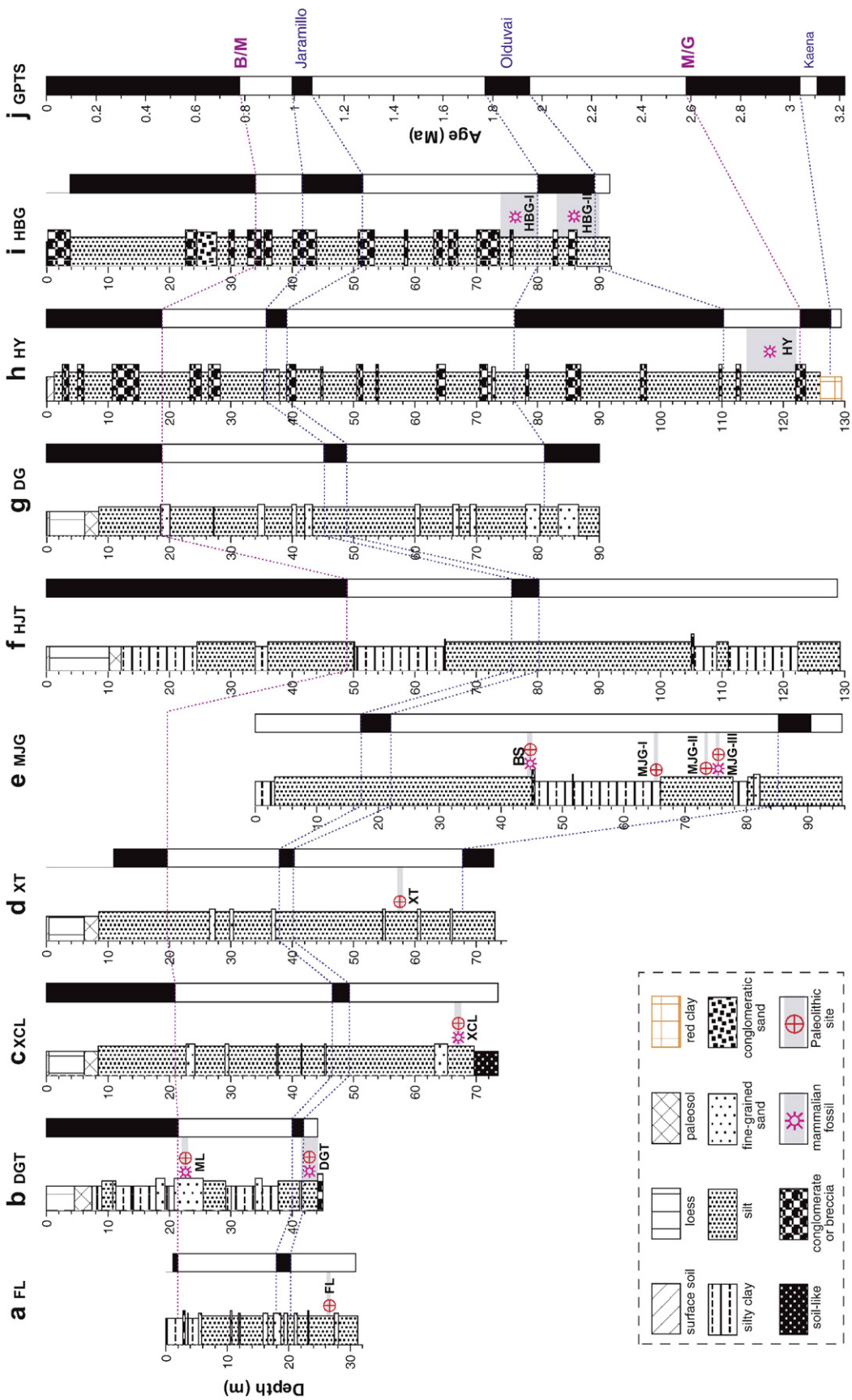

Figure 8. A synthetic diagram related the well-dated sections in the eastern Nihewan Basin, which contain early Pleistocene mammalian faunas and/or Paleolithic sites, to the geomagnetic polarity time scale (GPTS) (Berggren et al., 1995). Data sources of the lithostratigraphy and magnetostratigraphy: DGT (Li and Wang, 1982; Wang et al., 2005) and ML (Wang et al., 2005), FL (Deng et al., 2007), XCL (Zhu et al., 2001), XT (Deng et al., 2006), MJG and BS (Zhu et al., 2004), HJT (Zhu et al., 2004), DG (Zhu et al., 2001), HY and HBG (this study). B/M, Brunhes–Matuyama boundary. M/G, Matuyama–Gauss boundary. See the caption of Figure 1 for acronyms of the sections.

https://doi.org/10.1016/j.yqres.2007.10.006 Published online by Cambridge University Press

elements, about half of the mammalian genera have been found in those Nihewan faunas (see Table 1 and references; Tang, 1980; Tang and Ji, 1983; Li, 1984) and are magnetochronologically constrained between the onset of the Olduvai subchron and the Matuyama–Brunhes geomagnetic reversal. Thus, the faunal similarity leads us to estimate the age of the XSG fauna to be about 0.8–2.0 Ma.

Qiu (2000) carried out a systematic comparison between the XSG faunal elements and those of the Villafranchian age in Europe based on 20 commonly shared mammals at generic and/or specific level. He found that (1) eleven of the faunal elements (*Vulpes* sp., *Canis chihliensis*, *Canis chihliensis palmidens*, *Canis chihliensis minor*, *Ursus* cf. *U. etruscus*, *Pachycrocuta licenti*, *Chasmaporthetes* cf. *ossifragus*, *Megantereon nihowanensis*, *Homotherium* cf. *H. crenatidens*, *Sus* sp., *Eucladoceros boulei*) show close morphologic similarity with corresponding forms of the Olivola fauna in the early Villafranchian age, which was indirectly estimated to be ~1.8 Ma; (2) four of them (*Nyctereutes sinensis*, *Lynx shansius*, *Pseudodama elagans*, *Megalovis piveteaui*) may be compared with their counterparts of the Senèze fauna in the late Villafranchian age; and (3) two of them (*Borsodia chinensis*, *Meles chiai*) are possibly comparable with the Olivola faunal elements. The comparison led Qiu (2000) to conclude that the XSG fauna is chronologically close to the Olivola fauna in the early Villafranchian age. Therefore, chronological consensus of the XSG fauna has been reached separately, based on both magnetostratigraphic and biostratigraphic grounds.

Two mammalian faunas that are not yet well-dated are the DNG (Li, 1984) and DZ (Tang, 1980; Tang and Ji, 1983) faunas. The DNG fauna includes *Hyaena* sp., *Vulpes* sp., *Canis chihliensis minor*, *Meles chiai*, *Proboscidipparion sinensis*, *Equus sanmeniensis*, *Coelodonta antiquitatis*, *Gazella sinensis*, *Orientalomys nihowanicus*, and *Ochotona lagrelii minor* (Tang, 1980). The DZ fauna, also named Daodi–Dongyaozitou fauna (Wei, 1997), contains *Dipoides* sp., *Nyctereutes* cf. *sinensis*, *Lynx variabilis*, *Zygolophdon* sp., *Coelodonta antiquitatis*, *Proboscidipparion sinensis*, *Hipparion* cf. *houfenense*, *Paracamelus* sp., *Palaeotragus progressus*, *Antilospira yuxianensis*, *Gazella sinensis*, and *Axis* sp. (Tang, 1980; Tang and Ji, 1983). Most of the faunal elements present in the DNG and DZ faunas occur in the XSG fauna (Teilhard de Chardin and Piveteau, 1930), indicating a comparable age with that of the XSG fauna. In addition, the DNG fauna is stratigraphically higher than the

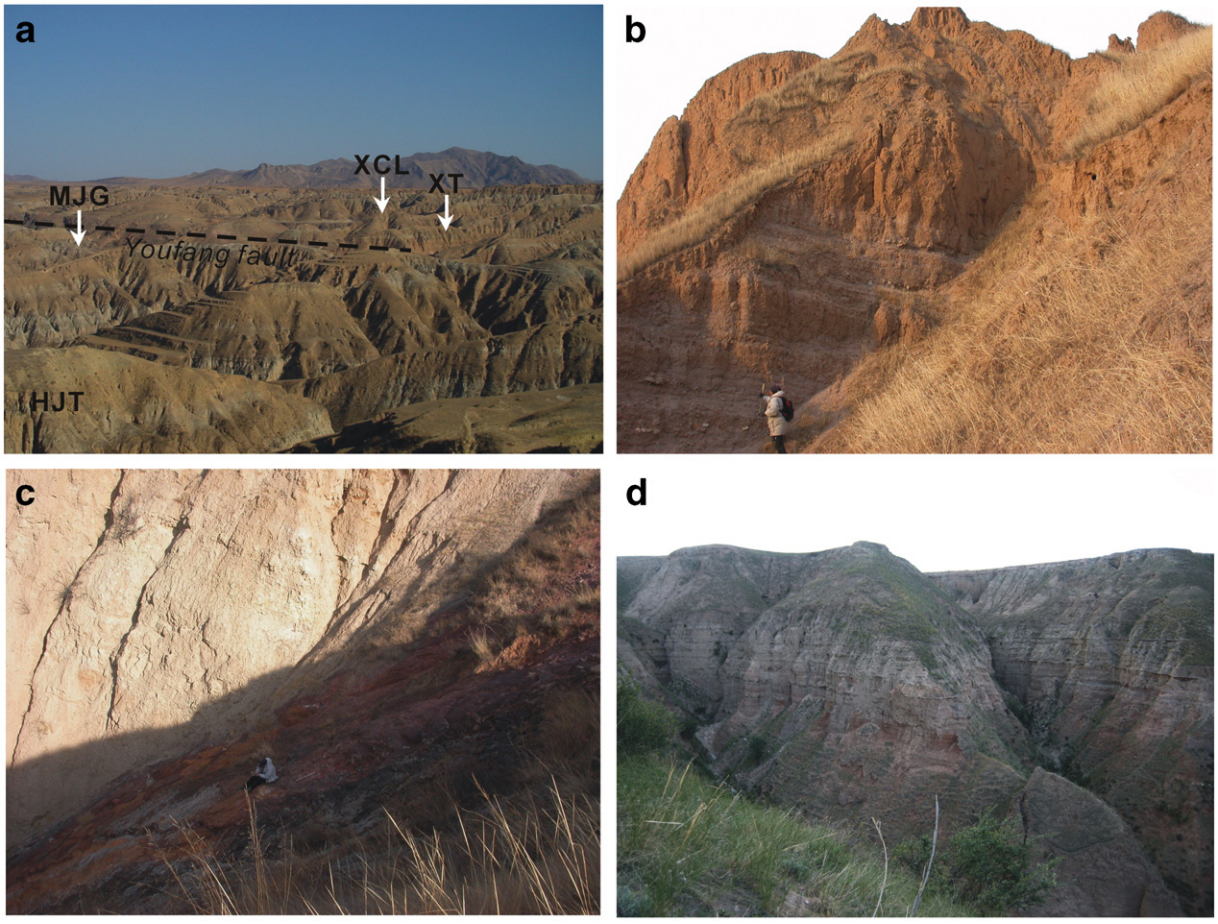

Figure 9. (a) Terrain of the eastern Nihewan Basin (Zhu et al., 2004), showing the approximate location of the XCL, MJG and XT Paleolithic sites, the HJT section, and the Youfang fault (dashed line). (b) A close view of the contact between the fluvio-lacustrine sediments and the last interglacial soil and the last glacial loess at Shixiali. (c) A close view of the contact between the Nihewan lacustrine sediments and the Youfang dip-slip fault just below the XCL Paleolithic site. (d) Outcrop of the HBG section.

https://doi.org/10.1016/j.yqres.2007.10.006 Published online by Cambridge University Press

Table 2
Faunal list of the Xiashagou (XSG) mammalian fauna (Teilhard de Chardin and Piveteau, 1930; Chen, 1988; Qiu, 2000) in the eastern Nihewan Basin

Taxa
Erinaceus cf. *dealbatus*
Borsodia chinensis
Vulpes sp.
Nyctereutes sinensis
Canis chihliensis
Canis chihliensis palmidens
Canis chihliensis minor
Ursus cf. *U. etruscus*
Meles chiai
Mustela pachygnatha
Lutra licenti
Pachycrocuta licenti
Chasmaporthetes cf. *ossifragus*
Megantereon nihowanensis
Homotherium cf. *H. crenatidens*
Sivapanthera pleistocaenicus
Lynx shansius
Palaeoloxodon namadicus
Postschizotherium chardini
Proboscidipparion sinensis
Equus sanmeniensis
Elasmotherium sp.
Coelodonta antiquitatis
Coelodonta sp.
Rhinoceros sinensis
Sus cf. *S. lydekkeri*
Paracamelus gigas
Elephas sp.
Cervulus cf. *sinensis*
Elaphurus bifurcatus
Pseudodama elagans
Eucladoceros boulei
Megalovis piveteaui
Gazella sinensis
Gazella subgutturosa
Spirocerus wongi
Antilope sp.
Ovis shantungensis
Bison palaeosinensis

DZ fauna (Li, 1984), and the DZ fauna has been suggested to be younger than the HBG fauna (Du, 1995; Wei, 1997). Therefore, the chronological order of the three faunas can be inferred: the DNG fauna was the youngest, the DZ fauna was in the middle, and the HBG fauna was the oldest. The HBG fauna includes two sub-faunas of HBG-I and HBG-II, which in this study have been placed in the post-Olduvai Matuyama chron (just above the upper boundary of the Olduvai subchron) and within the Olduvai subchron, respectively (Fig. 8). Presumably, the DNG and DZ faunas may be placed within the post-Olduvai Matuyama chron based upon the occurrence of some Tertiary survivors in the two faunas.

In summary, the Nihewan faunas have been placed between the Matuyama–Brunhes geomagnetic reversal and the onset of the Olduvai subchron, that is, between 0.78 Ma and 1.95 Ma. The Nihewan faunas conclusively spanned a range of time of about 0.8–2.0 Ma. Therefore, the combination of our new and previously published magnetostratigraphy has significantly refined the chronology of the terrestrial Nihewan faunas. As a result, the fossiliferous fluvio-lacustrine sequence in the eastern Nihewan Basin provides a key reference for the Plio–Pleistocene of North China with robust magnetochronological control.

Our magnetochronology for the Nihewan Formation also provides robust constraint on the ages of some specific faunal elements of particular paleoenvironmental and biochronological significance. For example, *Elephas* sp. in MJG-III Paleolithic site, magnetostratigraphically dated to be 1.66 Ma (Zhu et al., 2004), has been identified as the steppe mammoth *Mammuthus trogonthreii* (Wei and Lister, 2005). The MJG-III site therefore yields the globally oldest record of *Mammuthus trogonthreii*, significantly older than the formerly oldest records from Europe (1.0–0.8 Ma) and northeast Siberia (1.2–0.8 Ma) (Lister and Sher, 2001). The index fossil *Equus*, which was found in the sites of ML (~0.8 Ma) (Wang et al., 2005), DGT (~1.1 Ma) (Li and Wang, 1982; Wang et al., 2005), XCL (1.36 Ma) (Zhu et al., 2001), BS (1.32 Ma) (Zhu et al., 2004), MJG-III (1.66 Ma) (Zhu et al., 2004), XSG (0.8–2.0 Ma, this study) and DNG (<1.8 Ma, this study), occurred in the post-Olduvai Matuyama chron (<1.8 Ma) in the eastern Nihewan Basin. The fact agrees well with the previous concept that the taxon did not occur in Eurasia before ~2.6 Ma (Lindsay et al., 1980; Deng and Xue, 1999). Finally, the occurrence of *Canis* in the localities of DGT (~1.1 Ma) (Li and Wang, 1982; Wang et al., 2005), BS (1.32 Ma) (Zhu et al., 2004), HBG-II (1.8–2.0 Ma, this study), XSG (0.8–2.0 Ma, this study), and DNG (<1.8 Ma, this study) not only agrees well with the timing of the "Wolf" event (~1.7 Ma) (Azzaroli, 1983) but also suggests the close similarity between the Nihewan fauna (sensu stricto) and the Olivola fauna (Qiu, 2000).

Conclusions

This paper has synthesized new and recently published magnetostratigraphic data from the eastern Nihewan Basin to provide a chronological framework for the terrestrial Nihewan Formation and associated mammalian faunas. This synthesis significantly refines the geochronology of the fossiliferous fluvio-lacustrine sedimentary sequences exposed in the basin. The new magnetostratigraphic results show that the sequences at HY and HBG record the Brunhes chron, the Jaramillo and the Olduvai subchrons, and successive reverse polarity portions of the intervening Matuyama chron. The bottom of the sequence at HY can be extended to the late Gauss chron. As a result, the basal age of the Nihewan Formation in the eastern Nihewan Basin is constrained just prior to the Matuyama–Gauss geomagnetic reversal, that is, between ~2.6 Ma and ~3.0 Ma. The combined evidence of our new and previously published magnetochronological data suggests that the Nihewan Formation records the tectono-sedimentary processes of the Plio–Pleistocene Nihewan Basin.

The new magnetostratigraphic results significantly revise the chronology of the HY, HBG-I and HBG-II faunas, and show that the HY fauna is located in the pre-Olduvai Matuyama chron (1.95–2.58 Ma) and that the HBG-I and HBG-II faunas lie in the post-Olduvai Matuyama chron (1.07–1.77 Ma) and within

https://doi.org/10.1016/j.yqres.2007.10.006 Published online by Cambridge University Press

the Olduvai subchron (1.77–1.95 Ma), respectively. Coupled with our previously published magnetochronological data, the Nihewan faunas of the fluvio-lacustrine Nihewan Formation probably can be dated between the Matuyama–Brunhes geomagnetic reversal (0.78 Ma) and the onset of the Olduvai subchron (1.95 Ma), indicating that the Nihewan faunas spanned a range of time of about 0.8–2.0 Ma.

Acknowledgments

We are grateful to Dr. Xisheng Wang, an anonymous reviewer, Associate Editor Curtis Marean, and Editor Derek Booth for their insightful comments and suggestions to improve the manuscript. C. Deng thanks Drs. Tao Deng and Qingsong Liu for useful discussion. Paleomagnetic and mineral magnetic measurements were made in the Paleomagnetism and Geochronology Laboratory (SKL-LE), Institute of Geology and Geophysics, Chinese Academy of Sciences. Financial assistance was provided by NSFC (grants 40221402 and 40325011) and CAS.

References

Azzaroli, A., 1983. Quaternary mammals and the "end-Villafranchian" dispersal event — a turning point in the history of Eurasia. Palaeogeography, Palaeoclimatology, Palaeoecology 44, 117–139.

Barbour, G.B., 1924. Preliminary observation in Kalgan Area. Bulletin of the Geological Society of China 3, 167–168.

Barbour, G.B., 1925. The deposits of the Sankanho Valley. Bulletin of the Geological Society of China 4, 53–55.

Barbour, G.B., Licent, E., Teilhard de Chardin, P., 1927. Geological study of the deposits of the Sangkanho basin. Bulletin of the Geological Society of China 5 (2–4), 263–278.

Berggren, W.A., Kent, D.V., Swisher, C.C., Aubry, M.-P., 1995. A revised Cenozoic geochronology and chronostratigraphy in time scales and global stratigraphic correlations: a unified temporal framework for an historical geology. In: Berggren, W.A., Kent, D.V., Aubry, M.-P., Hardenbol, J. (Eds.), Geochronology, Timescales, and Stratigraphic Correlation. Special Publication, vol. 54. Society of Economic Paleontologists and Mineralogists, Tulsa, Oklahoma, pp. 129–212.

Chen, M.N., 1988. Study on the Nihewan Beds (in Chinese with English abstract). Ocean Press, Beijing, p. 143.

Day, R., Fuller, M., Schmidt, V.A., 1977. Hysteresis properties of titanomagnetites: grain-size and compositional dependence. Physics of the Earth and Planetary Interiors 13, 260–267.

Deng, T., Xue, X.X., 1999. Chinese Fossil Horses of *Equus* and their Environment. Ocean Press, Beijing, p. 158.

Deng, C.L., Vidic, N.J., Verosub, K.L., Singer, M.J., Liu, Q.S., Shaw, J., Zhu, R.X., 2005. Mineral magnetic variation of the Jiaodao Chinese loess/paleosol sequence and its bearing on long-term climatic variability. Journal of Geophysical Research 110, B03103. doi:10.1029/2004JB003451.

Deng, C.L., Wei, Q., Zhu, R.X., Wang, H.Q., Zhang, R., Ao, H., Chang, L., Pan, Y.X., 2006. Magnetostratigraphic age of the Xiantai Paleolithic site in the Nihewan Basin and implications for early human colonization of northeast Asia. Earth and Planetary Science Letters 244, 336–348.

Deng, C.L., Xie, F., Liu, C.C., Ao, H., Pan, Y.X., Zhu, R.X., 2007. Magnetochronology of the Feiliang Paleolithic site in the Nihewan Basin and implications for early human adaptability to high northern latitudes in East Asia. Geophysical Research Letters 34, L14301. doi:10.1029/2007GL030335.

Ding, Z.L., Sun, J.M., Liu, T.S., Zhu, R.X., Yang, S.L., Guo, B., 1998. Wind-blown origin of the Pliocene red clay formation in central Loess Plateau, China. Earth and Planetary Science Letters 161, 135–143.

Du, H.J., Cai, B.Q., Ma, A.C., 1995. Late Cenozoic biostratigraphic zone of Nihewan Basin (in Chinese with English abstract). Earth Science—Journal of China University of Geosciences 20, 35–42.

Flynn, L.J., Wu, W., Downs, W.R., 1997. Dating vertebrate microfaunas in the late Neogene record of northern China. Palaeogeography, Palaeoclimatology, Palaeoecology 133, 227–242.

Huang, W.P., Tang, Y.J., 1974. Observation on the later Cenozoic of Nihewan Basin. Vertebrata Palasiatica 12, 99–110.

Kirschvink, J.L., 1980. The least-squares line and plane and the analysis of palaeomagnetic data. Geophysical Journal of the Royal Astronomical Society 62, 699–718.

Li, Y., 1984. The early Pleistocene mammalian fossils of Danangou, Yuxian, Hebei. Vertebrata Palasiatica 22, 60–68.

Li, H.M., Wang, J.D., 1982. Magnetostratigraphic study of several typical geologic sections in North China. In: Liu, T.S. (Ed.), Quaternary Geology and Environment of China. Ocean Press, Beijing, pp. 33–38.

Lindsay, E.H., Opdyke, N.D., Johnson, N.M., 1980. Pliocene dispersal of *Equus* and the late Cenozoic mammalian dispersal events. Nature 287, 135–138.

Lister, A.M., Sher, A.V., 2001. The origin and evolution of the woolly mammoth. Science 294, 1094–1097.

Løvlie, R., Su, P., Fan, X.Z., Zhao, Z.J., Liu, C., 2001. A revised paleomagnetic age of the Nihewan Group at the Xujiayao Paleolithic Site, China. Quaternary Science Reviews 20, 1341–1353.

Min, L.R., Chi, Z.Q., 2003. Quaternary Geology of the Western Yangyuan Basin (in Chinese with English abstract). Geological Publishing House, Beijing, p. 160.

Qiu, Z.X., 2000. Nihewan fauna and Q/N boundary in China (in Chinese with English abstract). Quaternary Sciences 20, 142–154.

Schick, K.D., Toth, N., Wei, Q., Clark, J.D., Etler, D., 1991. Archaeological perspectives in the Nihewan Basin, China. Journal of Human Evolution 21, 13–26.

Tang, Y.J., 1980. Note on a small collection of early Pleistocene mammalian fossils from northern Hebei. Vertebrata Palasiatica 18, 314–323.

Tang, Y.J., Ji, H.X., 1983. A Pliocene–Pleistocene transitional fauna from Yuxian, northern Hebei. Vertebrata Palasiatica 21, 245–254.

Tang, Y.J., Li, Y., Chen, W.Y., 1995. Mammalian fossils and the age of Xiaochangliang paleolithic site of Yangyuan, Hebei (in Chinese with English abstract). Vertebrata Palasiatica 33, 74–83.

Teilhard de Chardin, P., Piveteau, J., 1930. Les mammiferes fossiles de Nihowan (Chine). Annales de Paleontologie 19, 1–134.

Teilhard de Chardin, P., Young, C.C., 1930. Preliminary observation on the pre-loessic and post-Ponian Formation in western Shansi and northern Shensi. Memoir Geological Survey China (Series A) 8, 1–54.

Wang, A.D., 1982. Discovery of the Pliocene mammalian faunas from the Nihewan region and its significance (in Chinese). Chinese Science Bulletin 27, 227–229.

Wang, X.S., Yang, Z.Y., Løvlie, R., Min, L.R., 2004. High-resolution magnetic stratigraphy of fluvio-lacustrine succession in the Nihewan Basin, China. Quaternary Science Reviews 23, 1187–1198.

Wang, H.Q., Deng, C.L., Zhu, R.X., Wei, Q., Hou, Y.M., Boëda, E., 2005. Magnetostratigraphic dating of the Donggutuo and Maliang Paleolithic sites in the Nihewan Basin, North China. Quaternary Research 64, 1–11.

Wang, H.Q., Deng, C.L., Zhu, R.X., Xie, F., 2006. Paleomagnetic dating of the Cenjiawan Paleolithic site in the Nihewan Basin, northern China. Science in China (Series D) 49, 295–303.

Wei, Q., 1985. Preliminary observation of Donggutuo palaeolithics (in Chinese). Acta Anthropologica Sinica 4, 289–300.

Wei, Q., 1991. Geologic sequence of the archaeological sites in the Nihewan Basin, North China (in Chinese with English abstract). In: Institute of Vertebrate Paleontology and Paleoanthropology (Ed.), Contributions to the XIII INQUA. Beijing Scientific and Technological Publishing House, Beijing, 1991, pp. 61–73.

Wei, Q., 1994. Banshan Paleolithic site from the Lower Pleistocene in the Nihewan Basin in northern China (in Chinese with English abstract). Acta Anthropologica Sinica 13, 223–238.

Wei, Q., 1997. The framework of archaeological geology of the Nihewan basin (in Chinese with English abstract). In: Tong, Y.S. (Ed.), Evidence of Evolution—Essays in Honor of Prof. Chungchien Young on the Hundredth Anniversary of His Birth. China Ocean Press, Beijing, pp. 193–207.

Wei, G.B., Lister, A.M., 2005. Significance of the dating of the Majuangou site for understanding Eurasian mammoth evolution (in Chinese with English abstract). Vertebrata Palasiatica 43, 243–244.
Xie, F., 2006. Nihewan. Cultural Relics Publishing House, Beijing, China, p. 330.
Xie, F., Li, J., Liu, L.Q., 2006. Paleolithic Archeology in the Nihewan Basin (in Chinese). Huashan Literature & Arts Press, Shijiazhuang, China, p. 278.
You, Y.Z., Tang, Y.J., Li, Y., 1980. Discovery of the Palaeoliths from the Nihewan Formation (in Chinese). Quaternaria Sinica 5, 1–11.
Young, C.C., 1950. The Plio–Pleistocene boundary in China. Report on 18th International Geological Congress, London, pp. 115–125.
Yuan, B.Y., Zhu, R.X., Tian, W.L., Cui, J.X., Li, R.Q., Wang, Q., Yan, F.H., 1996. Magnetostratigraphic dating on the Nihewan Formation (in Chinese). Science in China (Series D) 26, 67–73.
Zhou, T.R., Li, H.Z., Liu, Q.S., Li, R.Q., Sun, X.P., 1991. Cenozoic Paleogeography of the Nihewan Basin (in Chinese). Science Press, Beijing, p. 162.
Zhu, R.X., Hoffman, K.A., Potts, R., Deng, C.L., Pan, Y.X., Guo, B., Shi, C.D., Guo, Z.T., Yuan, B.Y., Hou, Y.M., Huang, W.W., 2001. Earliest presence of humans in northeast Asia. Nature 413, 413–417.
Zhu, R.X., An, Z.S., Potts, R., Hoffman, K.A., 2003. Magnetostratigraphic dating of early humans in China. Earth-Science Reviews 61, 341–359.
Zhu, R.X., Potts, R., Xie, F., Hoffman, K.A., Deng, C.L., Shi, C.D., Pan, Y.X., Wang, H.Q., Shi, R.P., Wang, Y.C., Shi, G.H., Wu, N.Q., 2004. New evidence on the earliest human presence at high northern latitudes in northeast Asia. Nature 431, 559–562.
Zhu, R.X., Deng, C.L., Pan, Y.X., 2007. Magnetochronology of the fluvio-lacustrine sequences in the Nihewan basin and implications for early human colonization of northeast Asia (in Chinese with English abstract). Quaternary Sciences 27, 922–944.
Zijderveld, J.D.A., 1967. A.C. demagnetization of rocks: analysis of results. In: Collinson, D.W., Creer, K.M., Runcorn, S.K. (Eds.), Methods in Paleomagnetism. Elsevier, New York, pp. 254–286.